

Lithium chloride ionic association in dilute aqueous solution: a constrained molecular dynamics study

Zhigang Zhang^a, Zhenhao Duan^{a,b,*}

^a Chinese Academy of Sciences, Institute of Geology and Geophysics, Beijing 100029, China

^b Department of Chemistry, University of California, 0340/9500 Gilman Dr., San Diego, La Jolla, CA 92129, USA

Received 12 August 2003; accepted 24 October 2003

Abstract

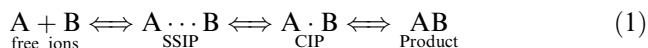
Constrained molecular dynamics simulations were carried out to investigate the lithium chloride ionic associations in dilute aqueous solutions over a wide temperature range. Solvent mediated potentials of mean force have been carefully calculated at different thermodynamic conditions. Two intermediate states of ionic association can be well identified with an energy barrier from the oscillatory free energy profile. Clear pictures for the microscopic association structures are presented with a remarkable feature of strong hydration effect of lithium ion and the bridging role of its hydrating complex. Experimental association constants have been reasonably reproduced and a general trend of the increasing ionic association at high temperatures and low densities was observed. Additional simulations with different numbers of water molecules have been performed to check the possible artifacts introducing from periodic and finite size effects and confirm the reliability of our simulation results. Marginal differences of the simulated curves are believed to result from the significant compensation and canceling effect between the bare ionic forces and solvent induced mean force. Finally we confirmed the importance of accurate descriptions of dielectric properties of solvent in the ionic association study.

© 2003 Elsevier B.V. All rights reserved.

1. Introduction

Ionic association and speciation is of fundamental importance in the chemical processes related to aqueous electrolyte solutions [4,16]. It has been an interesting subject with various attempts including experiments, theoretical and semi-empirical approaches over the last several decades. Early attempts with continuum models of solvent have successfully predicted the diffusion-controlled and long-ranged properties of the rapid ionic reactions with very small barriers [5]. From the primitive continuum models and the experiments of electrolyte conductance [36,37,48,55,74], we know that all electrolytes in dilute aqueous solutions have a general trend to associate or even form stable neutral ion pairs [51] at high temperatures and low pressures due to the decreasing dielectric screening effect, which is prominently regulated by the dielectric constant of water.

In order to investigate the ionic association with more detailed information of the ionic short-range properties, more complicated microscopic descriptions with water molecule explicit models are needed. Based on these models, the scheme proposed by Fuoss [62] and Winstein [72] turns out to be especially useful in the understanding of the ionic association mechanism:



in which A and B represent two ions (Li^+ and Cl^- in this study) in the aqueous solutions and the two intermediate states are defined in the process of dissolving the salt product (AB) into free ions ($A + B$): a contact ion pair (CIP: $A \cdot B$) and a solvent separated ion pair (SSIP: $A \cdots B$). These intermediate states have been identified through the increasingly accurate experiments using infrared and Raman spectroscopy techniques [25,27,33,64]. However, these kinds of experimental measurements are still limited in the sub-critical region and encounter many difficulties in providing detailed structures and inter-conversion dynamics.

* Corresponding author. Tel.: +858-8220281; fax: +858-4843899.
E-mail address: duanzhenhao@yahoo.com (Z. Duan).

In the study of ionic association, computer simulation acts as a peculiar role between the pure theoretical approaches and experiments. On one hand, it can be regarded as a well-established statistical model with least empirical assumptions and can be utilized to check the validities of many other theoretical approaches. On the other hand, more importantly, it is actually a kind of “computer experiment” which is straightforward in the interpreting of the properties of molecule explicit systems and provides a supplementary solution to the problems of experiments with detailed information from normal to extreme conditions. Through computer simulations, the SSIP state described above can be well distinguished from the CIP state with a noticeable barrier indicated by the oscillatory solvent mediated potential of mean force (pmf) and hence the relevant microscopic structures and interconversion dynamics can be well revealed.

Potential of mean force is actually the free energy surface along the chosen coordinate and it incorporates solvent effects as well as the intrinsic interaction between the two particles [47]. It is of great importance in the study of ionic association and has been extensively investigated in recent years with Ornstein–Zernike-like integration methods [35,38,45,54,59] and computer simulation techniques [3,7,11,13,30,63,65]. Although the integration methods require far less computer time and the ongoing progresses make it possible to obtain pmfs even with a three dimensional structure [45], the results are still approximate and sometimes may yield pmfs with diminished or even erroneous structures [11,29,40]. Consequently, we prefer molecular dynamics simulations as a relatively rigorous solution of the full statistical mechanical problem with the aid of super-computational power.

Since the problems of poor sampling can be delicately solved by such techniques as free energy perturbation [43], umbrella sampling [70], thermodynamic integration [49], and constrained molecular dynamics [15], a number of publications have come forth with the computer simulation results of pmfs for various alkali halides in dilute aqueous solutions [3,7,13,30,63,65]. However, there still exist some confusions. For instance, although the Ewald summation method is superior to the cutoff truncation methods [10,53,66], the periodicity introduced by the periodic boundary conditions may lead to undesirable effects in the simulation of solutions [41]. These effects on the ionic pmfs have not yet carefully checked with computer simulations. So, further investigations are still justified.

In this study, we focus on the lithium chloride ionic association in dilute aqueous solutions. The lithium chloride is selected since it is a representative member of alkali halide but has surprisingly received far less attention with regard to its association/dissociation properties on the molecular level. We hope this study

can provide some complementary results for experiment and may be helpful for theoretical and semi-empirical treatment of the aqueous solutions [2,21]. Moreover, we hope some relevant confusions described above can be properly clarified through the discussions of our simulation results.

In the next section, theoretical backgrounds for the constrained molecular dynamics and characterizations of the ionic association are briefly discussed. Subsequently, simulation details with potential models and program setups are presented. Then simulation results are presented and carefully discussed. Finally, some conclusions are drawn.

2. Theoretical background

2.1. Constrained molecular dynamics

A straightforward way to calculate the ionic mean force potential $W(r)$ is through the ionic radial distribution function $g(r)$:

$$W(r) = -k_B T \ln(g(r)), \quad (2)$$

where k_B is the Boltzmann constant, T is the temperature of the system.

However, in the dilute aqueous systems, a simple molecular dynamics simulation would always result in a problematic ionic radial distribution function for the sake of inadequate sampling or some traps during the propagation of the configurations. In order to solve this problem, more sophisticated sampling methods are needed, such as free energy perturbation [43], umbrella sampling method [70] and weighted histogram analysis method [46,60]. Constrained molecular dynamics, which was proposed by Ciccotti and his coworkers [12,15], introduces an alternative routine and is nowadays widely utilized as a rigorous and versatile tool to study the free energy profile [68] and relevant properties [58].

Constrained molecular dynamics methodology in the study of interionic potential of mean force actually can be regarded as a special case of the popular thermodynamic integration method [49], which has the following form:

$$W(\lambda_2) - W(\lambda_1) = \int_{\lambda_1}^{\lambda_2} \left\langle \frac{\partial H}{\partial \lambda'} \right\rangle_{\lambda'} d\lambda', \quad (3)$$

where λ_1 and λ_2 corresponds to the initial and final state, respectively, W is the free energy, H is the Hamiltonian of the system, $\langle \rangle_{\lambda'}$ is the conditional average of an ensemble corresponding to the coupling parameter λ' . Minus the integrand in Eq. (3) is called the *thermodynamic mean force* [20,52]. Eq. (3) can be read as the difference of the free energy of two states equals to the negative integral of thermodynamic mean force between these two states. When we are interested in the ionic

potential of mean force, the coupling parameter is actually the interionic distance r and in this simple case the thermodynamic mean force is equivalent to the *constraint mean force* [52,68], which is denoted as $F(r)$. Then Eq. (3) becomes:

$$W(r) = W(r_0) - \int_{r_0}^r F(r') dr' \quad (4)$$

and r_0 is the interionic distance of a reference state.

Eq. (4) is the basic formula of constrained molecular dynamics. A rigorous deducing process of this equation from Eq. (2) with statistical theories can be found in the paper of [15], which in the mean time reveals a clearer physical background of the ionic mean force and is very helpful for our programming and computations. According to their analysis, the ionic mean force in a system of N water molecules and two ions (A and B) can be calculated from:

$$F(r) = \frac{1}{2} \langle \hat{r}_{AB} \cdot (\vec{F}_A - \vec{F}_B) \rangle_r^{\text{cond}}, \quad (5)$$

where $\hat{r}_{AB} = (\vec{r}_A - \vec{r}_B)/r_{AB}$ is the unit vector from ion A to ion B; \vec{F}_A and \vec{F}_B are the total forces acting on the two ions, respectively; $\langle \rangle_r^{\text{cond}}$ represents the conditional statistical average corresponding to a interionic distance of r . Note that in the constrained molecular dynamics, not only the interionic distance should be fixed at r , but also the relative velocity between the two ions should be zero [15,39], that is, $\vec{v}_{AB} \cdot \vec{r}_{AB} \equiv 0$.

2.2. Characterizations of the ionic association

As the salt product does not exist in the aqueous solutions, we rewrite Eq. (1) below as the multistep mechanism of ionic association in solution:



Two equilibrium constants (K_1 and K_2) are involved. If we define $A : B \equiv A \cdots B + A \cdot B$ as *pairing ions*, then there is an additional equilibrium constant K_a , which characterizes the equilibrium between free ions and pairing ions. These three constants are related with the following equation:

$$K_a = K_1 + K_1 K_2. \quad (7)$$

In many cases and also in this paper, K_a and K_2 are interested since K_a is related to the electrical conductance that can be measured through well established experiments [28,36,37] and K_2 reveals the delicate balance between the ionic interaction and the effect of water molecules surrounding the ions. We substitute K_2 with another equivalent notation K_e below for consistence with other documents. These equilibrium constants can all be calculated from the solvent mediated ionic potential of mean force.

Define α as the degree of dissociation, then $1 - \alpha$ features the possibility of ionic pairing ($A : B$). The association equilibrium constant K_a can be expressed as:

$$K_a = \frac{(1 - \alpha)\gamma_{A:B}}{c_0 \alpha^2 \gamma_{\pm}^2}, \quad (8)$$

where $\gamma_{A:B}$ is the activity coefficient of related ions, γ_{\pm} is the mean activity coefficient of the free ions, c_0 is the initial concentration of the salt [16]. From the statistical mechanical interpretation [13], α is given by:

$$\alpha = 1 - 4\pi c_0 \int_0^{r_m} \exp(-[W(r)/k_B T]) r^2 dr, \quad (9)$$

where r_m is the geometric limit for association and distinguish the SSIPs from free ions. According to [13], r_m can be selected as the second maximum of the simulated pmf (i.e., it encompasses the CIP and SSIP configurations). In the infinite dilute limit, $c_0 \rightarrow 0$, $\gamma_{A:B} \approx \gamma_{\pm}^2 \approx 1$, so from Eqs. (8) and (9),

$$\begin{aligned} K_a &= \lim_{c_0 \rightarrow 0} \frac{1 - \alpha}{c_0 \alpha^2} \\ &= \lim_{c_0 \rightarrow 0} \frac{4\pi \int_0^{r_m} \exp(-W(r)/k_B T) r^2 dr}{(1 - 4\pi c_0 \int_0^{r_m} \exp(-W(r)/k_B T) r^2 dr)^2} \\ &= 4\pi \int_0^{r_m} \exp(-W(r)/k_B T) r^2 dr. \end{aligned} \quad (10)$$

In order to calculate another equilibrium constant, K_e , a transition state with an interionic separation of r^{\ddagger} is identified. It is corresponding to the maximum free energy barrier in the interconversion process between CIP and SSIP states. K_e can be calculated from:

$$K_e = \frac{\int_{r^{\ddagger}}^{r_m} \exp(-[W(r)/k_B T]) r^2 dr}{\int_0^{r^{\ddagger}} \exp(-[W(r)/k_B T]) r^2 dr}, \quad (11)$$

where the numerator and the denominator are proportional to the concentrations of SSIP and CIP configurations, respectively [13,15].

3. Simulation details

It is well known that the solvent mediated ionic potential of mean force is sensitive to the interaction potential model [19,63]. This urges us to carefully select an appropriate set of potential models and parameters. SPCE (extended simple point charge) [6] model was adopted to feature the water molecules for its accurate description of the dielectric constant over a wide range of temperatures and pressures [56,71]. Ion–water interaction was modeled as the Coulombic interactions plus short-ranged Lennard–Jones potential between the ions and oxygen or hydrogen atoms of water molecules [13], i.e.,

$$u_{\text{IW}} = \sum_{\beta=1}^3 \left\{ \frac{q_1 q_{\beta}}{r_{1\beta}} + 4\epsilon_{1\beta} \left[\left(\frac{\sigma_{1\beta}}{r_{1\beta}} \right)^{12} - \left(\frac{\sigma_{1\beta}}{r_{1\beta}} \right)^6 \right] \right\}, \quad (12)$$

where β represents an interaction site (hydrogen or oxygen atom) on a water molecule, q_1 and q_{β} are the electric charges, $r_{1\beta}$ is the distance between the ion and the interaction site. $\epsilon_{1\beta}$ and $\sigma_{1\beta}$ are the Lennard–Jones parameters which have been given in [54] and also can be found in Table 1. For the ionic interaction potential, the popular Huggins–Mayer form was adopted:

$$u_{ij} = \frac{q_i q_j}{r_{ij}} + B_{ij} e^{-r_{ij}/\rho_{ij}} - \frac{C_{ij}}{r_{ij}^6}, \quad (13)$$

where q_i and q_j are the electric charges on two ions, r_{ij} is their separation and B_{ij} , ρ_{ij} , C_{ij} are the parameters given in Table 1 [54].

It can be seen from Eq. (4) that a series of simulations are needed to obtain an accurate profile of solvent mediated ionic mean force potential. A single simulation corresponds to a fixed interionic separation. We did about 22 simulations with various ionic separations from 1.8 to 7.0 Å with intervals of 0.2–0.3 Å for each physical state. Note that 7.0 Å was selected as the reference state since it is practically infeasible in the finite size simulations to select a state with infinite ionic separation. It can be assumed that the interionic mean force potential at the reference state is essentially the same as the prediction by primitive continuum theory [15,30], i.e., in this study,

$$W(r_0 = 7.0) \approx \frac{q_A q_B}{\epsilon r_0}, \quad (14)$$

where q_A and q_B are the electric charges of the ions, ϵ is the dielectric constant of the solvent. This will inevitably introduce some errors into the calculated association constant K_a [13] but will surely not affect the oscillatory shape of pmf curves and the equilibrium constant K_e .

All the simulations were performed in the canonical ensemble (constant-NVT). The temperature was kept at 298, 573 or 1073 K, which represent ambient, near critical and supercritical conditions, respectively. Density effects on the lithium chloride ionic association were investigated by changing the simulation box size from 35.98 a.u. (corresponding to 1.0 g/cm³) to 39.84 a.u.

(0.74 g/cm³). There were 230 water molecules, a lithium ion and a chloride ion in the simulation box. The conventional periodic boundary conditions and minimum image conventions [1] were used in the simulations to treat out-of-box atoms and to calculate inter-atom distances. Long-range electrostatic forces and energies were calculated with the Ewald summation procedure to avoid some possible erroneous artifacts [3,10,53,66]. The time step of all the simulations was set as 0.75 fs. Interionic separation and the geometry of water molecules were constrained with the algorithm described in [61]. An extended version of Verlet algorithm [9,73] was used to propagate the isothermal trajectory. Energy and momentum conservations were carefully checked during the trajectory. The instantaneous mean force (Eq. (5)) was recorded and counted into the statistical average for about 120–200 ps after a 20–30 ps pre-equilibrium stage of the system.

4. Results and discussions

4.1. Static dielectric constant

From Eq. (14), the potential of mean force beyond certain interionic separation can be assessed by the primitive continuum theory with the static dielectric constant of water. Nevertheless, an accurate description of the dielectric properties of water turns out to be nontrivial due to a slow reorientational rate in the hydrogen bond network [32].

In this study, the dielectric constant was calculated from:

$$\epsilon = \frac{4\pi}{3k_B T V} \langle \vec{M}^2 \rangle, \quad (15)$$

where \vec{M} is the total box dipole moment, V is the volume of the simulation box, bracket $\langle \rangle$ denotes the statistical average [65]. Pure water systems at the same temperatures and densities of corresponding aqueous solutions were involved to exclude the perturbation of ions. At the ambient condition, 298 K and 1.0 g/cm³, an extremely long trajectory of 600 ps yielded an average dielectric constant of 65.4, which is smaller than the experimental value of 78.3 [8] but consistent with prior publications [56,65]. Increasing temperature and decreasing density significantly reduce the computational time [71], which can be seen from the cumulative average of dielectric constant during the propagation of the trajectory at 573 K and 0.74 g/cm³ shown in Fig. 1. It can be seen that about 120 ps of simulation time is sufficient to obtain a good statistical estimation in this case. Simulated dielectric constants with SPCE model at different conditions and corresponding experimental data are listed in Table 2. Uncertainties were calculated by analyzing the collected data (discarding the pre-equilibrium stage)

Table 1
Parameters for ion–water and ion–ion interaction potential

| | $\epsilon_{1\beta}$ | $\sigma_{1\beta}$ | |
|----------------------------------|---------------------|-------------------|----------|
| Li ⁺ –O | 0.1439 | 2.28 | |
| Li ⁺ –H | 0.1439 | 0.87 | |
| Cl [−] –O | 0.3598 | 3.55 | |
| Cl [−] –H | 0.3598 | 2.14 | |
| | B_{ij} | ρ_{ij} | C_{ij} |
| Li ⁺ –Cl [−] | 7482.8 | 0.342 | 28.78 |

Note. Energies in kcal/mol, distances in Å.

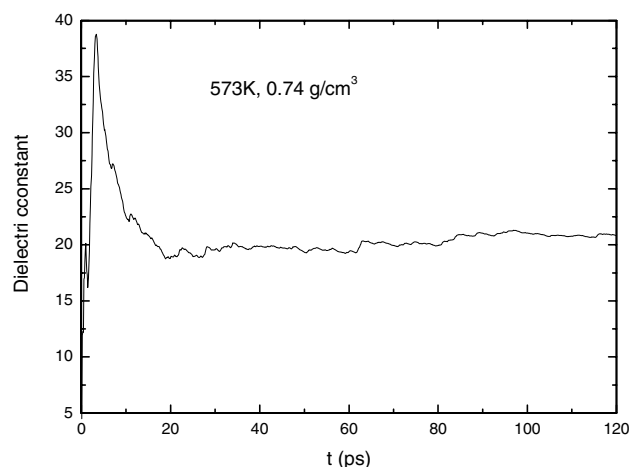


Fig. 1. Cumulative average of dielectric constant during the propagation of the trajectory for SPCE water at 573 K and 0.74 g/cm³.

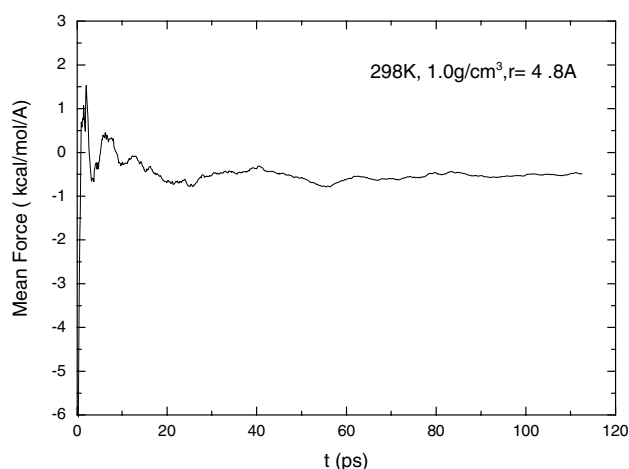


Fig. 2. Monitoring the convergence of interionic mean force from the cumulative average.

Table 2

Simulated dielectric constants with SPCE model at different conditions and corresponding experimental data

| | Simulated | Experiment |
|--------------------------------|------------|-------------------|
| 298 K, 1.0 g/cm ³ | 65.4 ± 4.6 | 78.3 ^a |
| 573 K, 1.0 g/cm ³ | 32.1 ± 1.6 | 33.2 ^b |
| 573 K, 0.74 g/cm ³ | 20.6 ± 0.6 | 21.5 ^b |
| 1073 K, 0.74 g/cm ³ | 8.9 ± 0.2 | 8.4 ^c |

^a Ref. [8].

^b Ref. [34].

^c Prediction in [26].

with the method described in Appendix A. These results demonstrate the remarkable ability of SPCE water model in the prediction of the dielectric properties of water over wide temperatures and pressures and this is essential for the reliable calculation of pmfs.

4.2. Lithium chloride association

According to Eq. (5), interionic mean force was estimated from the time average of the projection onto the interionic axis of the instantaneous total force exerted on the ions along the constrained molecular dynamics trajectory. During the calculations, the convergence of interionic mean force was carefully monitored with a cumulative average plot of the mean force (Fig. 2). Table 3 summarizes the calculated mean forces for different interionic separations. Uncertainties in the parentheses were evaluated with comprehensive analyses over the instantaneous recorded mean force data (discarding the pre-equilibrium stage) (Appendix A).

Potential of mean force were calculated by Eqs. (4) and (14) and plotted in Fig. 3. A common feature of these curves in Fig. 3 is that they are oscillatory with two minima and an obvious saddle maximum. Since potential of mean force is actually a kind of free energy profile

[47], this feature distinguishes the ionic association into two well-defined sub-states of ionic association (CIP and SSIP) with an interconversion barrier and verifies the association mechanism proposed by Fuoss and Winstein (Eq. (1)).

Table 4 summarizes main characteristics of these pmf curves and also the association constants (K_a and K_e) from Eqs. (10) and (11) with carefully checked uncertainties (Appendix B). From Fig. 3 and Table 4, we notice that the interconversions between CIP and SSIP configurations are asymmetric: the energy barriers are

Table 3

Calculated mean forces for different interionic separations

| r (Å) | 298 K 1.0 g/cm ³ | 573 K 1.0 g/cm ³ | 573 K 0.74 g/cm ³ | 1073 K 0.74 g/cm ³ |
|---------|--------------------------------|--------------------------------|---------------------------------|----------------------------------|
| 1.8 | 59.40(.22) | 51.53(.19) | 48.66(.23) | 41.40(.10) |
| 2.0 | 25.83(.16) | 20.57(.16) | 19.62(.23) | 11.69(.22) |
| 2.2 | 7.42(.12) | 4.57(.08) | 4.11(.17) | -2.76(.18) |
| 2.5 | -3.15(.06) | -5.03(.07) | -5.10(.09) | -8.28(.13) |
| 2.8 | -5.17(.14) | -4.46(.21) | -5.38(.17) | -7.34(.22) |
| 3.0 | 1.64(.20) | -0.26(.23) | -1.32(.22) | -4.39(.14) |
| 3.2 | 6.65(.13) | 3.43(.19) | 2.93(.18) | -2.19(.15) |
| 3.5 | 5.80(.13) | 4.42(.10) | 4.68(.12) | 0.77(.22) |
| 3.8 | 4.23(.14) | 3.68(.17) | 3.86(.11) | 2.01(.12) |
| 4.0 | 2.63(.09) | 2.93(.17) | 2.69(.13) | 1.69(.17) |
| 4.2 | 1.71(.16) | 1.60(.14) | 1.53(.18) | 1.06(.17) |
| 4.5 | 0.59(.10) | 0.85(.15) | 0.26(.18) | -0.07(.11) |
| 4.8 | -0.52(.12) | -0.19(.16) | -0.54(.21) | -0.69(.18) |
| 5.0 | -1.12(.19) | -1.02(.17) | -1.19(.16) | -1.45(.11) |
| 5.2 | -1.54(.16) | -1.56(.15) | -2.12(.13) | -2.21(.07) |
| 5.5 | -0.47(.16) | -0.79(.14) | -1.53(.09) | -2.33(.12) |
| 5.8 | 0.34(.08) | -0.29(.16) | -0.36(.09) | -1.59(.08) |
| 6.0 | 0.37(.15) | 0.12(.15) | 0.01(.07) | -1.15(.13) |
| 6.2 | -0.19(.14) | -0.19(.13) | 0.09(.07) | -0.84(.08) |
| 6.5 | 0.25(.08) | 0.18(.07) | 0.19(.12) | -0.46(.14) |
| 6.8 | -0.39(.12) | 0.02(.12) | 0.09(.06) | -0.34(.15) |
| 7.0 | -0.07(.12) | 0.00(.11) | -0.22(.04) | -0.23(.14) |

Note. All the mean force data in unit of kcal/mol/Å. The numbers in the parentheses are the uncertainties in the simulations. For example, 41.40(.10) means 41.40 ± 0.10.

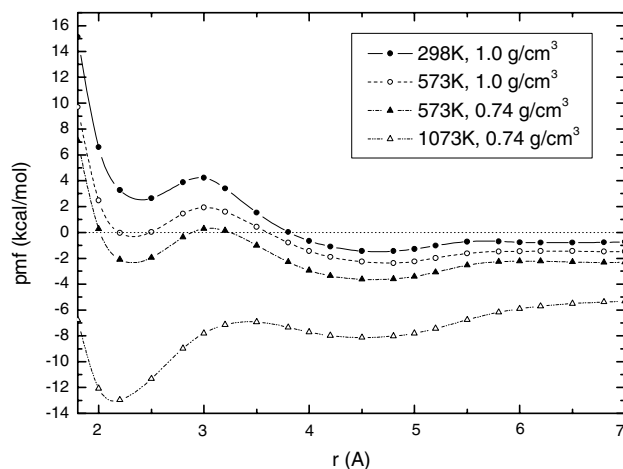


Fig. 3. Lithium chloride interionic potential of mean force at different temperatures and densities.

unequal between the dissolving process of CIP \rightarrow SSIP and the reverse one, meanwhile the former process becomes more and more difficult with increasing energy barrier at higher temperature and lower density while the latter shows an opposite trend. At temperatures below 573 K and densities larger than 0.74 g/cm^3 , the valley of SSIP is deeper than that of CIP; while at 1073 K and 0.74 g/cm^3 the valley of CIP is deeper than that of SSIP with an energy difference of about 4.8 kcal/mol.

It is more convenient to use $1/(1 + K_e)$ as an indication of the relative concentration of ion pairs in CIP state, as shown in Fig. 4. According to this figure, percentage of CIP configurations becomes larger as the increasing of temperatures and decreasing of densities but always less than that of SSIP. At low temperatures and high densities, SSIP configurations are remarkably prominent with a percentage more than 97%. At the ambient condition, CIP state almost disappears with a trivial percentage of less than 0.01%. This can be utilized to explain why the LiCl contact ion pair has not yet been found at dilutions through experiments [23].

Experimental association constants of K_a at dilutions are available with conductance experiments [36,37, 48,50,74]. Nevertheless, the published association constants are not always consistent with each other, which can be clearly shown in Fig. 5.

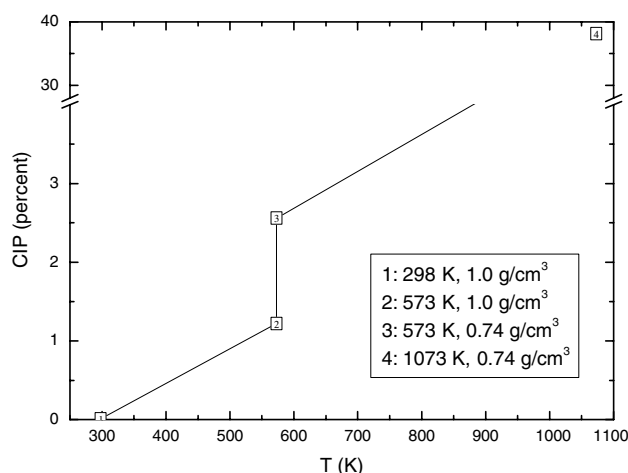


Fig. 4. Relative concentration of ion pairs in CIP state at different thermodynamic conditions.

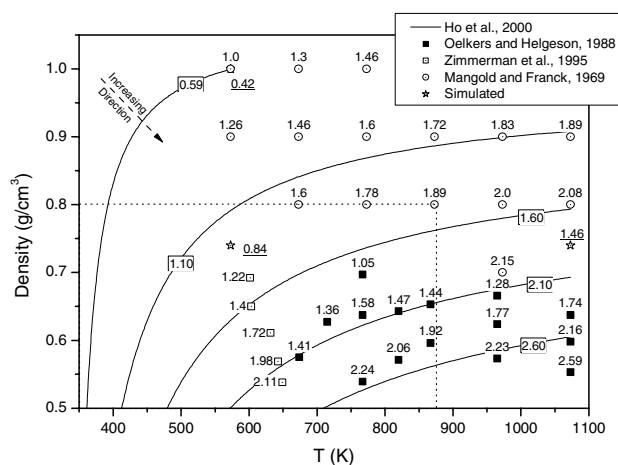


Fig. 5. Lithium chloride ionic association constants $\log K_a^M$ from experimental based calculations [36,48,50,74] and simulations in this study. Figures near the symbols represent the values of $\log K_a^M$ at corresponding state while those rounded with a rectangle denote the values for the contours (solid line), which are calculated with Eq. (16).

According to the experiments and calculations in [36], molar unit of K_a can be estimated from the following equation:

Table 4
Main characteristics of lithium chloride ionic association and pmfs at dilution

| | $\log K_a$ | $\log K_e$ | $r_{\min 1}$ | r^\ddagger | $r_{\min 2}$ | r_m | CIP \rightarrow SSIP barrier | SSIP \rightarrow CIP barrier |
|-----|------------|------------|--------------|--------------|--------------|-----------|--------------------------------|--------------------------------|
| I | 0.39(.08) | 3.99(.08) | 2.50 | 3.00 | 4.70(.14) | 5.73(.13) | 1.60(.04) | 5.68(.08) |
| II | 0.42(.08) | 1.91(.08) | 2.20 | 3.00 | 4.80(.01) | 6.20(.22) | 1.96(.06) | 4.29(.10) |
| III | 0.84(.03) | 1.58(.03) | 2.20 | 3.00 | 4.55(.11) | 6.03(.09) | 2.39(.06) | 3.93(.09) |
| IV | 1.46(.02) | 0.21(.02) | 2.20 | 3.50 | 4.50 | 6.99(.01) | 6.04(.09) | 1.21(.07) |

Note. I, 298 K, 1.0 g/cm^3 ; II, 573 K, 1.0 g/cm^3 ; III, 573 K, 0.74 g/cm^3 ; IV, 1073 K, 0.74 g/cm^3 ; K_a and K_e in l/mol ; distances in Å; energies in kcal/mol; $r_{\min 1}$, r^\ddagger , $r_{\min 2}$ and r_m denote the first minimum, first maximum, second minimum and second maximum, respectively; the numbers in the parentheses are the uncertainties, e.g., 0.35(.03) means 0.35 ± 0.03 .

$$\log K_a^M = 0.920 - 189.93/T - (12.507 - 4283.2/T) \log \rho, \quad (16)$$

where T is the temperature in K and ρ is the density in g/cm^3 . We plotted the contours of $\log K_a^M$ in Fig. 5 for convenience of comparison. Note that the contours are reliable only in the region of 323–873 K and 0.3–0.8 g/cm^3 (indicated by dotted line) [36], those out of this region can be regarded as predictions or extrapolations. Association constants from other publications [48,50,74] are also shown in this figure. By comparisons, data from [74] are approximately consistent with those of [36] but cover a limited thermodynamic region. Estimations by [48,50] show noticeable deviations. For example, at 674 K and 0.575 g/cm^3 [50] estimated $\log K_a^M = 1.41$, which significantly lower than the value of 2.12 calculated from Eq. (16). In contrast, [48] overestimated the association constants by 0.3–0.6 logarithmic units compared with [36]. This kind of inconsistency can be attributed to the difference of experimental conditions and more importantly to the calculation procedure based on different assumptions [42].

Also indicated in Fig. 5 are our simulated lithium chloride ionic association constants at three different thermodynamic conditions. Simulated ionic association constants increases as the increasing of temperatures and the decreasing of densities, which is consistent with the trend of the experimental association constant. We notice that our simulated results can be well merged into the profile of the calculations by [50]. Compared with [48], simulated association constants are essentially underestimated by about 0.5–0.6 logarithmic units. The association constants calculated by [36] are found to be intermediate between these two sets of data. At 573 K and 0.74 g/cm^3 , from Eq. (16) the association constant is estimated to be 1.25 or so, which is 0.41 logarithmic units higher than the simulated results. Although the prediction behavior of Eq. (16) at temperatures higher than 873 K or densities larger than 1.0 g/cm^3 has not yet confirmed, we would like to get the extrapolations to 573 K, 1.0 g/cm^3 and 1073 K, 0.74 g/cm^3 as a rough estimation. The simulated results are again smaller than the corresponding estimations by Eq. (16) with 0.15–0.4 logarithmic units.

Considering inconsistency of experimental based calculations described above and the uncertainty in Eq. (16) itself ($\delta \log K_a^M \approx \pm 0.2$), our simulation results are reasonably consistent with experiments.

From the recorded instantaneous configurations during the constrained molecular dynamics simulations, the detailed structures of lithium chloride association can be disclosed by introducing a cylindrical coordinate system [15]. As shown in Fig. 6, the x -axis is selected to pass through the mass center of the ion pairs with an origin located at the midpoint of the interionic separation. The

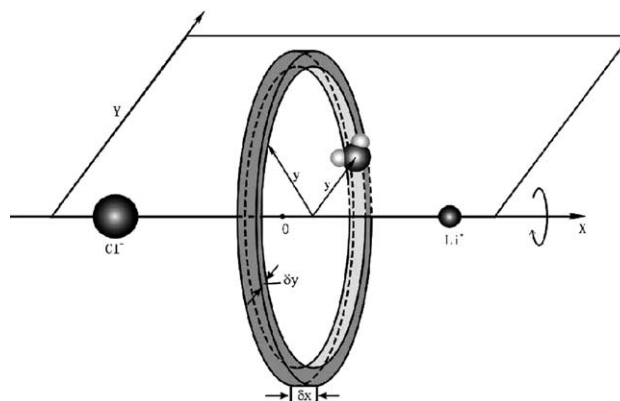


Fig. 6. The cylindrical coordinate system established for the contour plots of the water molecule density profiles.

densities of oxygen and hydrogen in the vicinity of ion pairs can be computed by an imaginary plane rotated around the x -axis. Each time the plane is determined by the mass center of the interested atom. The number density $n(x, y)$ is defined as the statistical average of the number $N(x, y)$ of atoms in the cylindrical unit shell (indicated in Fig. 6), i.e.,

$$n(x, y) = \frac{\langle N(x, y) \rangle}{2\pi y \cdot \delta y \cdot \delta x}. \quad (17)$$

Fig. 7 provides a clear picture of lithium chloride association structure with the contour of the densities of oxygen and hydrogen atoms at three ionic separations representing CIP, transition state (position of the first maximum) and SSIP, respectively. Corresponding snapshot is also shown on the top right window of each plot. At CIP state ($r = 2.2 \text{ \AA}$), each ion occupies the expected hydration position of another ion and noticeably chloride ion forms a well-defined tetrahedron around lithium ion along with another three water molecules. At high temperatures and low densities of dilute solutions, this kind of structure for ionic association will dominate and as a result we can consider the electrolyte as stable neutral ion pairs [51], which is helpful for the theoretical and semi-empirical treatment of the aqueous solutions [2]. When the interionic separation is enlarged to the transition state ($r = 3.0 \text{ \AA}$), the disturbance of the ions over each other is reduced. The water molecules near lithium ion begin to form a distorted tetrahedral hydration shell. However, the transition state complex is not stable for the sake of saddle point of free energy profile. At SSIP state ($r = 4.5 \text{ \AA}$), a well-defined tetrahedral structure of lithium hydration shell is identified. At the same time, one of the hydrating water molecules interacts directly with the chloride ion and can be defined as a bridging molecule. We can imagine at concentrated aqueous solutions lithium ion and its hydrating water molecules would “bridge” two neighboring chloride ions and this can be utilized to

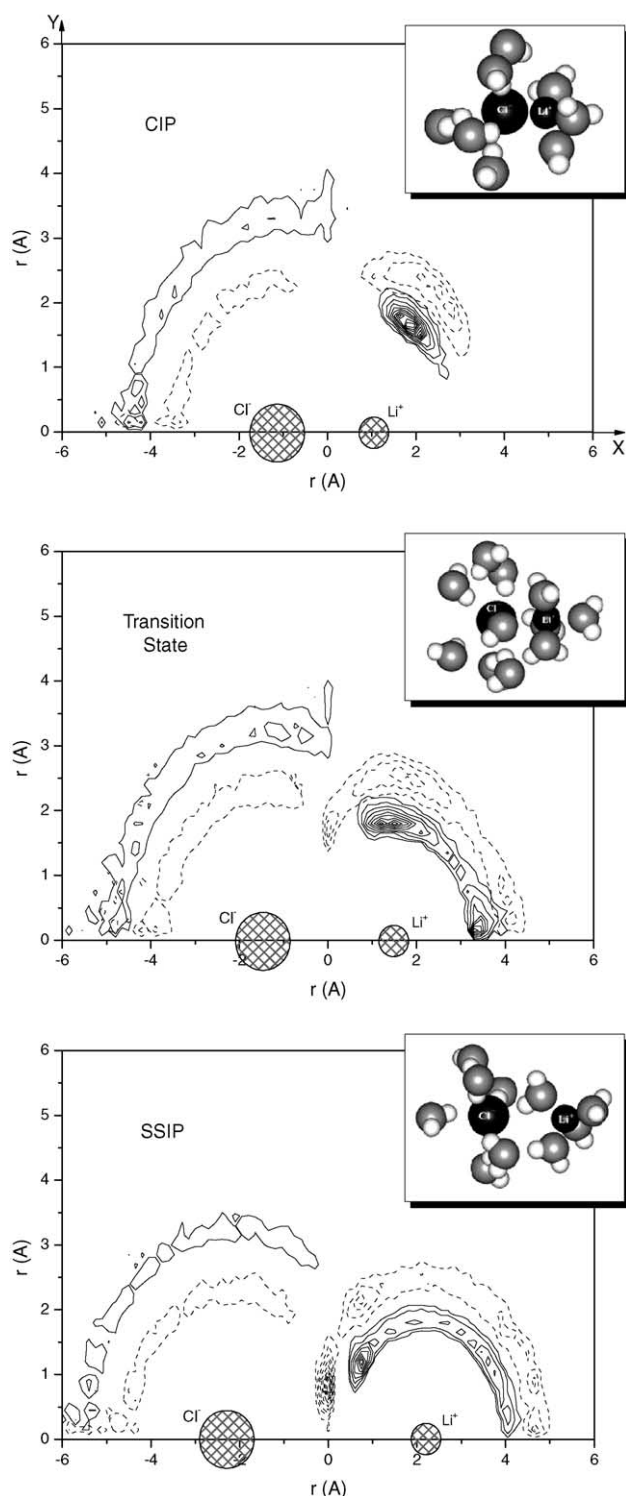


Fig. 7. Lithium chloride association structures at 573 K and 0.74 g/cm^3 revealed from the oxygen (solid) and hydrogen (dash) density contours and typical snapshots (top right window) at different ionic separations: CIP, $r = 2.2 \text{ Å}$; transition state, $r = 3.0 \text{ Å}$; SSIP, $r = 4.5 \text{ Å}$.

explain the experimental derived two peaks in the chloride–chloride pair correlation function at high concentrations [17]. Link the above described pictures,

the dynamics of lithium chloride microscopic association can be reasonably deduced with a $\text{CIP} \rightleftharpoons \text{SSIP}$ interconversion mechanism consistent with those suggested by former researchers [44,58].

4.3. Finite size effects

Treatment of long-ranged electrostatic interactions turns out to be essential for the reliability of the simulated properties [10]. Ewald summation handles the electrostatic forces with excellent mathematical treatment [1] and appears to be promising and superior to many other efficient techniques in view of some possible erroneous artifacts [3,18]. However, Ewald technique may also introduce some errors originated from the volume dependent finite-size and periodicity effects [24,67]. In the computer simulation of ionic mean force potential, it has long been believed that the boundary conditions distort the real physical background of the interested systems [69]. We noticed several obvious distortions: (1) the simulated aqueous solution cannot be infinitely dilute even with a single ion pair for the perturbations of their periodic replicas; (2) the simulated interaction between ion pairs with a separation of half of the simulation box and parallel to the box edge would be zero while it is not the case for the solely interacting ion pairs, which is finite until they are separated by an infinite distance. These distortions may introduce some undesirable effects. [41] have extensively investigated the nature and magnitude of periodicity-induced artifacts based on continuum electrostatics. In the following descriptions, we will show that with further analysis on the constrained molecular dynamics simulation results we can check the finite size effects from the explicit-solvent system and confirm the reliability of our simulation results.

We have performed additional simulations with different numbers of water molecules (108 and 460) under the same condition of the previous simulations (573 K and 0.74 g/cm^3). The simulated pmf curves are shown in Fig. 8 with marginal differences of less than 0.5 kcal/mol .

Since the ionic separation is fixed during a specific simulation, the bare (i.e., without solvent molecules) interionic force, which is denoted as $F_{\text{bare}}(r)$, can be conveniently separated from the total mean force [15] and we can rewrite Eq. (5) as:

$$F(r) = F_{\text{bare}}(r) + \Delta F(r), \quad (18a)$$

$$\Delta F(r) = \frac{1}{2} \left\langle \hat{r}_{\text{AB}} \cdot (\vec{F}_{\text{AW}} - \vec{F}_{\text{BW}}) \right\rangle_r^{\text{cond}}, \quad (18b)$$

where \vec{F}_{AW} and \vec{F}_{BW} are forces on ions exerted by the water molecules and $\Delta F(r)$ denotes the solvent contribution to the interionic mean force. Note that in Eqs. (18a) and (18b) $F_{\text{bare}}(r)$ includes the interactions from

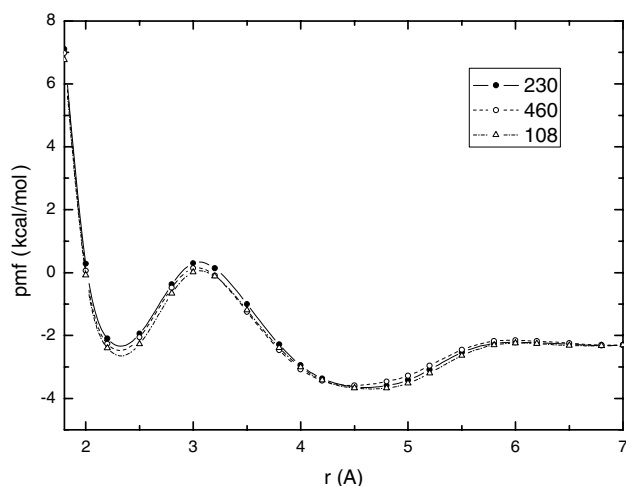


Fig. 8. Marginal finite size effects shown by the comparison of pmf curves with different amounts of sampled water molecules (108, 230 and 460).

the ionic periodic replicas in addition to the direct interaction between the central ion pair.

Fig. 9 shows this kind of treatments of the mean forces in the systems with different numbers of water molecules. Fig. 9(a) represents the finite-size effects of the periodic systems in vacuum. When the system size is increased, the bare interionic force would approach the direct force (between a sole ion pair) limit, as indicated by the dashed arrow in Fig. 9(a). Obviously, the difference between the finite system and the infinite counterpart cannot be ignored at large ionic separations. If the molecular distribution around ions is replaced by an isotropic continuous solvent with high dielectric constant, the difference would be significantly reduced by the dielectric screening effect from the simple continuum electrostatics. [41] took the solvation effects into their considerations and found a large compensation between the perturbations of the Coulomb and solvation contributions. Fig. 9 reveals an analogical compensation effect between the bare ionic forces and solvent induced mean forces. This compensation effect significantly cancels the finite-size effect, as shown in Fig. 8. Moreover, the explanation described above can be used to extrapolate with limited uncertainties the simulated pmf curves to those at infinite dilution, which would finally be liberated from the volume dependent finite size effects.

4.4. Perspective

It is well known that the simulated pmf curves are sensitive to the interaction potential model. Ionic potential of mean forces for a number of alkali halides have been published with dramatic difference or even inconsistency, which can be attributed to the variance of the selected potential models besides some possible

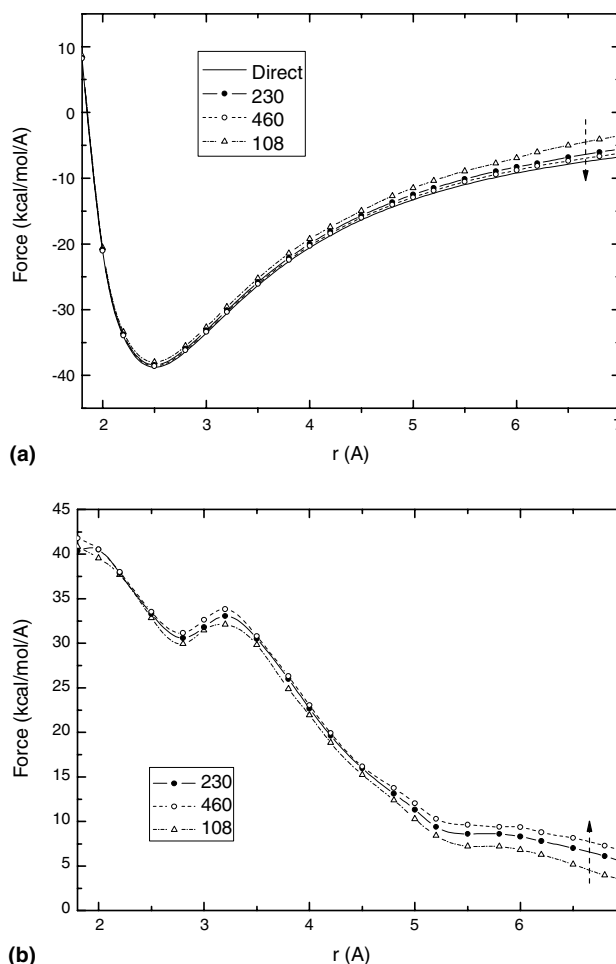


Fig. 9. Compensation between the finite size effects from the contributions of bare ions and surrounding water molecules. (a) Bare ionic mean force at different periodic systems; (b) solvent contributions to the interionic mean force.

oversimplifications in the simulations [3,7,13,30,63,65]. In our opinion, not all of these published pmfs are credible or even physical. When we select the solvent potential model, we should emphasize the reasonable description of dielectric properties of solvent. [14] highlighted this point by reducing the errors introduced from dielectric constant (Eq. (14)) in the calculation of the association constant. We would like to go further with a test of another solvent potential model below.

We replaced the SPCE water with RWK2 [57] water and restarted simulations with input setups unchanged. RWK2 water model yields remarkably good predictions of steam, liquid water and ice and liquid–vapor phase equilibrium [22] but significantly underestimates the dielectric constant, which is about 27.4 at ambient condition and 10.9 at 573 K and 0.74 g/cm^3 according to our simulation in this study. Fig. 10 shows the simulated pmf curve at 573 K and 0.74 g/cm^3 in a dot-solid line. According to this curve, CIP is much more stable than SSIP. This is obviously inconsistent with the experi-

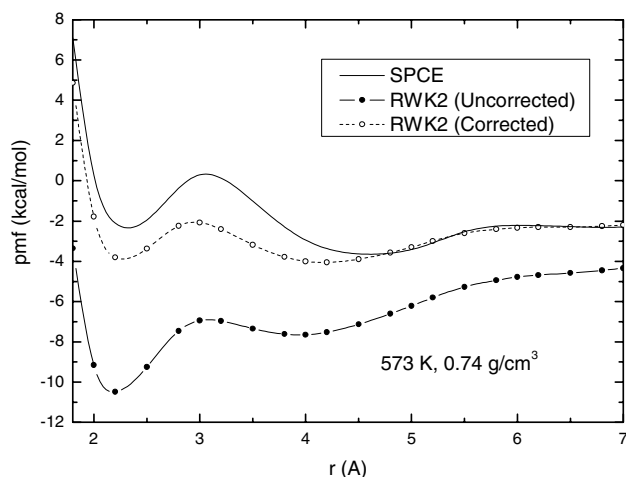


Fig. 10. Simulated pmf with RWK2 model at 573 K and 0.74 g/cm³ and an approximate correction (mentioned in the text) to it.

mental results. We present an approximate correction method analogous to that suggested in [54]:

$$W'(r) = \frac{q_A q_B}{\epsilon_{\text{exp}} r_0} - \int_{r_0}^r F(r') dr' + \left(\frac{1}{\epsilon_{\text{model}}} - \frac{1}{\epsilon_{\text{exp}}} \right) \times \int_{r_0}^r F_{\text{bare}}(r') dr', \quad (19)$$

where ϵ_{model} and ϵ_{exp} represent the dielectric constant of model and experiment, respectively. Corrected mean force potential curve is shown in Fig. 10 as a circle-dash line, which is comparable with that of SPCE model and seems reasonable with an association constant $\log K_a^M \approx 1.07$. This is roughly consistent with experiments.

Of course, we should also mention here that the correction method presented here is not strict since the dielectric properties in the vicinity of ions would be quite different with that of bulk and the treatment of short-ranged interactions with an isotropic dielectric constant obviously oversimplifies the microscopic properties. So it is important to choose a potential model with reasonable descriptions of dielectric properties of solvent.

5. Conclusion

Lithium chloride ionic associations in dilute aqueous solutions have been extensively investigated through the constrained molecular dynamics simulations. Solvent mediated potentials of mean force have been carefully calculated at different thermodynamic conditions. Intensive analyses over the simulated results indicate: (1) two intermediate states of association of Li⁺ and Cl[−] (CIP andSSIP) can be well identified with an energy barrier from the oscillatory free energy profile and the pictures of corresponding microscopic structures reveal the strong hydration effect of lithium ion and hence the

remarkable bridge role of the lithium ion hydrating complex; (2) the interconversions between CIP andSSIP are asymmetric with a trend of the former gradually becoming prominent as the increasing of temperature and decreasing of density; (3) with carefully selected interaction potentials the simulations reasonably reproduce experimental association constants and show a general trend of increasing association effect at high temperatures and low densities.

In order to confirm the reliability of our simulated results, additional simulations with different numbers of water molecules have been performed to check the possible artifacts introducing from periodic and finite size effects. Marginal differences of the simulated curves are believed to result from the significant compensation and canceling effect between the bare ionic forces and solvent induced mean force. As a result, the simulated pmf curves seem to be independent of the simulation sizes.

Acknowledgements

We would like to thank Drs. John Weare and G. Ciccotti for his valuable discussions. This work is supported by Zhenhao Duan's 'Hundred Scientists Project' funds awarded by the Chinese Academy of Sciences and his Outstanding Young Scientist Funds (#40225008) awarded by National Science Foundation of China. This work is also partially supported by the National Science Foundation (USA): Ear-0126331.

Appendix A. Error estimation in equilibrium averages

It is well known that the estimated errors can be efficiently reduced through long enough statistics. For the slow-convergent properties, such as the dielectric constant of water and mean force in this study, the estimated errors are very important to verify the reliabilities of the statistical average. We briefly introduce the evaluation method for estimated errors below. The interested reader is referred to [1] for details.

Consider some property X , the run average $\langle X \rangle_{\text{run}}$ and variance $\sigma^2(\langle X \rangle_{\text{run}})$ are calculated by:

$$\langle X \rangle_{\text{run}} = \frac{1}{\tau_{\text{run}}} \sum_{\tau=1}^{\tau_{\text{run}}} X(\tau), \quad (\text{A.1})$$

$$\sigma^2(\langle X \rangle_{\text{run}}) = \frac{\sigma^2(X)}{\tau_{\text{run}}}, \quad (\text{A.2})$$

where τ_{run} is the statistic times and

$$\sigma^2(X) = \frac{1}{\tau_{\text{run}}} \sum_{\tau=1}^{\tau_{\text{run}}} (X(\tau) - \langle X \rangle_{\text{run}})^2. \quad (\text{A.3})$$

Eq. (A.2) is only valid by assuming each instantaneous $X(\tau)$ were statistically independent of the others. In the practical statistics, a correlation time (or statistical inefficiency) s_{run} should be evaluated with:

$$s_{\text{run}} = \lim_{\tau_b \rightarrow \infty} \frac{\tau_b \sigma^2(\langle X \rangle_b)}{\sigma^2(X)} \quad (\text{A.4})$$

by dividing the whole length τ_{run} into n_b blocks ($n_b \tau_b = \tau_{\text{run}}$) and

$$\langle X \rangle_b = \frac{1}{\tau_b} \sum_{\tau=1}^{\tau_b} X(\tau), \quad (\text{A.5})$$

$$\sigma^2(\langle X \rangle_b) = \frac{1}{n_b} \sum_{b=1}^{n_b} (\langle X \rangle_b - \langle X \rangle_{\text{run}})^2. \quad (\text{A.6})$$

The final estimated error in the run average $\langle X \rangle_{\text{run}}$ can be calculated as:

$$\delta_X = \left[\frac{s_{\text{run}}}{\tau_{\text{run}}} \sigma^2(X) \right]^{1/2}. \quad (\text{A.7})$$

For an interested property X , s_{run} and $\sigma^2(X)$ are essentially independent with simulation length τ_{run} . So the estimated error can be reduced with the elongation of the simulation length with a proportion of $1/\tau_{\text{run}}^{1/2}$.

Appendix B. Estimations of the uncertainties in pmf and relevant properties

In calculations of mean force potential and relevant properties (association constants, positions of extrema, energy barriers, etc.) errors are inevitably introduced from the uncertainties in the estimation of mean forces and dielectric constants. Since the integral limits in Eqs. (10) and (11) are also related to these uncertainties, we prefer the following numerical method to the analytical assessment [31]. It is analogous to the method suggested by [13].

From the previous simulations and analyses, we get the dielectric constant $\langle \epsilon \rangle_{\text{run}} \pm \delta_\epsilon$ and a series of mean force data $\langle F(r) \rangle_{\text{run}} \pm \delta_{F(r)}$. δ_ϵ and $\delta_{F(r)}$ are the estimated errors with the method mentioned in Appendix A.

- (I) Generate random values of ϵ_{ran} and $F(r)_{\text{ran}}$, which obey Gaussian distributions centered at $\langle \epsilon \rangle_{\text{run}}$ and $\langle F(r) \rangle_{\text{run}}$ with variances of δ_ϵ^2 and $\delta_{F(r)}^2$, respectively.
- (II) The potential of mean force was calculated by Eqs. (4) and (14) with these random-generated dielectric constant and mean force data.
- (III) Positions of the extrema were determined for the integral limit in Eqs. (10) and (11). Relevant properties were subsequently calculated and counted into statistics.

The process described above (from I to III) was repeated over 20,000 times and the final uncertainties in the relevant properties were considered to be their standard deviations in the sampling statistics.

References

- [1] M.P. Allen, D.J. Tildesley, Computer simulation of liquids, Oxford Science Publications (1989).
- [2] A. Anderko, K.S. Pitzer, Equation of state representation of phase equilibria and volumetric properties of the system NaCl–H₂O above 573 K, *Geochim. Cosmochim. Acta* 57 (1993) 1657.
- [3] J.S. Bader, D. Chandler, Computer simulation study of the mean forces between ferrous and ferric ions in water, *J. Phys. Chem.* 96 (1992) 6423.
- [4] H.L. Barnes, Geochemistry of hydrothermal ore deposits, John Wiley & Sons. (1997).
- [5] A.C. Belch, M. Berkowitz, J.A. McCammon, Solvation structure of a sodium chloride ion pair in water, *J. Am. Chem. Soc.* 108 (1986) 1755.
- [6] H.J.C. Berenden, J.R. Grigera, T.P. Straatsma, The missing term in effective pair potentials, *J. Phys. Chem.* 91 (1987) 6269.
- [7] M. Berkowitz, O.A. Karim, J.A. McCammon, P.J. Rossky, Sodium chloride ion pair interaction in water: computer simulation, *Chem. Phys. Lett.* 105 (1984) 577.
- [8] D. Bertolini, M. Cassettari, G. Salvetti, The dielectric relaxation time of supercooled water, *J. Chem. Phys.* 76 (1982) 3285.
- [9] D. Brown, J.H.R. Clarke, A comparison of constant energy, constant temperature and constant pressure ensembles in molecular dynamics simulations of atomic liquids, *Mol. Phys.* 51 (1984) 1243.
- [10] M. Brunsteiner, S. Boresch, Influence of the treatment of electrostatic interactions on the results of free energy calculations of dipolar systems, *J. Chem. Phys.* 112 (2000) 6953.
- [11] J.K. Buckner, W.L. Jorgensen, Energetics and hydration of the constituent ion pairs of tetramethylammonium chloride, *J. Am. Chem. Soc.* 111 (1988) 2507.
- [12] E.A. Carter, G. Ciccotti, J.T. Hynes, R. Kapral, Constrained reaction coordinate dynamics for the simulation of rare events, *Chem. Phys. Lett.* 156 (1989) 472.
- [13] A.A. Chialvo, P.T. Cummings, H.D. Cochran, J.M. Simonson, R.E. Mesmer, Na⁺–Cl[−] ion pair association in supercritical water, *J. Chem. Phys.* 103 (1995) 9379.
- [14] A.A. Chialvo, P.T. Cummings, J.M. Simonson, R.E. Mesmer, Temperature and density effects on the high temperature ionic speciation in dilute Na⁺/Cl[−] aqueous solutions, *J. Chem. Phys.* 105 (1996) 9248.
- [15] G. Ciccotti, M. Ferrario, J.T. Hynes, R. Kapral, Constrained molecular dynamics and the mean potential for an ion pair in a polar solvent, *Chem. Phys.* 129 (1989) 241.
- [16] B.E. Conway, Ionic hydration in chemistry and biophysics, Elsevier Scientific Publishing Co, 1981.
- [17] A.P. Copestake, G.W. Neilson, J.E. Enderby, The structure of a highly concentrated aqueous solution of lithium chloride, *J. Phys. C: Solid State Phys.* 18 (1985) 4211.
- [18] L.X. Dang, B.M. Pettitt, Chloride ion pairs in water, *J. Am. Chem. Soc.* 109 (1987) 5531.
- [19] L.X. Dang, B.M. Pettitt, P.J. Rossky, On the correlation between like ion pairs in water, *J. Chem. Phys.* 96 (1991) 4046.
- [20] E. Darve, A. Pohorille, Calculating free energies using average force, *J. Chem. Phys.* 115 (2001) 9169.
- [21] Z. Duan, N. Moller, J.H. Weare, Equation of state for the NaCl–H₂O–CO₂ system: prediction of phase equilibria and volumetric properties, *Geochim. Cosmochim. Acta* 59 (1995) 2869.
- [22] Z. Duan, N. Moller, J.H. Weare, Molecular dynamics simulation of water properties using RWK2 potential: from clusters to bulk water, *Geochim. Cosmochim. Acta* 59 (16) (1995) 3273.
- [23] J.E. Enderby, S. Cummings, G.J. Herdman, G.W. Neilson, P.S. Salmon, N. Skipper, Diffraction and the study of aqua ions, *J. Phys. Chem.* 91 (1987) 5851.

- [24] F.E. Figueirido, G.S. Del-Buono, R.M. Levy, On finite-size effects in computer simulations using the Ewald potential, *J. Chem. Phys.* 103 (1995) 6133.
- [25] G. Fleissner, A. Hallbrucker, E. Mayer, Increasing contact ion pairing in the supercooled and glassy states of dilute aqueous magnesium, calcium, and strontium nitrate solution: implications for biomolecules, *J. Phys. Chem.* 97 (1993) 4806.
- [26] E.U. Franck, S. Rosenzweig, M. Christoforakos, Calculation of the dielectric constant of water to 1000 °C and very high pressures, *Ber. Bunsenges. Phys. Chem.* 94 (1990) 199.
- [27] J.L. Goodman, K.S. Peters, Picosecond decay dynamics of the *trans*-stilbene-olefin contact ion pair: electron-transfer vs. ion-pair separation, *J. Am. Chem. Soc.* 107 (1985) 6459.
- [28] M.S. Gruskiewicz, R.H. Wood, Conductance of dilute LiCl, NaCl, NaBr, and CsBr solutions in supercritical water using a flow conductance cell, *J. Phys. Chem. B* 101 (1997) 6549.
- [29] E. Guardia, R. Rey, J.A. Padro, $\text{Na}^+ - \text{Na}^+$ and $\text{Cl}^- - \text{Cl}^-$ ion pairs in water: mean force potentials by constrained molecular dynamics, *J. Chem. Phys.* 95 (1991) 2823.
- [30] E. Guardia, R. Rey, J.A. Padro, Potential of mean force by constrained molecular dynamics: a sodium chloride ion-pair in water, *Chem. Phys.* 155 (1991) 187.
- [31] E. Guardia, R. Rey, J.A. Padro, Statistical errors in constrained molecular dynamics calculations of the mean force potential, *Mol. Simul.* 9 (1992) 201.
- [32] Y. Guissani, B. Guillot, A computer simulation study of liquid-vapor coexistence curve of water, *J. Chem. Phys.* 98 (1993) 8221.
- [33] W. Hage, A. Hallbrucker, E. Mayer, Increasing ion pairing and aggregation in supercooled and glassy dilute aqueous electrolyte solution as seen by FTIR spectroscopy of alkali metal thiocyanates, *J. Phys. Chem.* 96 (1992) 6488.
- [34] K. Heger, M. Uematsu, E.U. Franck, The static dielectric constant of water at high pressures and temperatures to 500 MPa and 550 °C, *Ber. Bunsenges. Phys. Chem.* 84 (1980) 758.
- [35] F. Hirata, P.J. Rossky, An extended RISM equation for molecular polar fluids, *Chem. Phys. Lett.* 83 (1981) 329.
- [36] P.C. Ho, H. Bianchi, D.A. Palmer, R.H. Wood, Conductivity of dilute aqueous electrolyte solutions at high temperatures and pressures using a flow cell, *J. Sol. Chem.* 29 (2000) 217.
- [37] P.C. Ho, D.A. Palmer, Determination of ion association in dilute aqueous lithium chloride and lithium hydroxide solutions to 600 °C and 300 MPa by electrical conductance measurements, *J. Chem. Eng. Data* 43 (1998) 162.
- [38] G. Hummer, D.M. Soumpasis, An extended RISM study of simple electrolytes: pair correlations in a NaCl-SPC water model, *Mol. Phys.* 75 (1992) 633.
- [39] G. Hummer, D.M. Soumpasis, M. Neumann, Pair correlations in a NaCl-SPC water model: simulations versus extended RISM computations, *Mol. Phys.* 77 (1992) 769.
- [40] G. Hummer, D.M. Soumpasis, M. Neumann, Computer simulations do not support Cl-Cl pairing in aqueous NaCl solution, *Mol. Phys.* 81 (1993) 1155.
- [41] P.H. Hunenberger, J.A. McCammon, Ewald artifacts in computer simulations of ionic solvation and ion-ion interaction: a continuum electrostatics study, *J. Chem. Phys.* 110 (1999) 1856.
- [42] K. Ibuki, M. Ueno, M. Nakahara, Analysis of concentration dependence of electrical conductances for 1:1 electrolytes in sub- and supercritical water, *J. Phys. Chem.* 104 (2000) 5139.
- [43] W.L. Jorgensen, J.K. Buckner, S. Boudon, J. Tirado-Reeves, Efficient computation of absolute free energies of binding by computer simulations: applications to the methane dimer in water, *J. Chem. Phys.* 89 (1988) 3742.
- [44] O.A. Karim, J.A. McCammon, Dynamics of a sodium chloride ion pair in water, *J. Am. Chem. Soc.* 108 (1986) 1762.
- [45] A. Kovalenko, F. Hirata, Potential of mean force of simple ions in ambient aqueous solution. I Three-dimensional reference interaction site model approach, *J. Chem. Phys.* 112 (2000) 10391.
- [46] S. Kumar, D. Bouzida, R.H. Swendsen, P.A. Kollman, J.M. Rosenberg, The weighted histogram analysis method for free-energy calculations on biomolecules. I. The method, *J. Comput. Chem.* 13 (1992) 1011.
- [47] A.R. Leach, *Molecular Modelling: Principles and Applications*, Longman, 1996.
- [48] K. Mangold, E.U. Franck, Electrical conductance of aqueous solutions at high temperatures and pressures, II[1]. Alkalichloride in water to 1000 °C and 12 kbar, *Ber. Bunsen-Ges. Phys. Chem.* 73 (1969) 21.
- [49] M. Mezei, D.L. Beveridge, Free energy simulations, *Ann. NY Acad. Sci.* 482 (1986) 1.
- [50] E.H. Oelkers, H.C. Helgeson, Calculation of the thermodynamic and transport properties of aqueous species at high pressures and temperatures: dissociation constants for supercritical alkali metal halides at temperatures from 400 to 800 °C and pressures from 500 to 4000 bar, *J. Phys. Chem.* 92 (1988) 1631.
- [51] E.H. Oelkers, H.C. Helgeson, Calculation of activity coefficients and degrees of formation of neutral ion pairs in supercritical electrolyte solutions, *Geochim. Cosmochim. Acta* 55 (1991) 1235.
- [52] W.K.D. Otter, W.J. Briels, The calculation of free-energy differences by constrained molecular-dynamics simulations, *J. Chem. Phys.* 109 (1998) 4139.
- [53] L. Perera, U. Essmann, M.L. Berkowitz, Effect of the treatment of long-range forces on the dynamics of ions in aqueous solutions, *J. Chem. Phys.* 102 (1995) 450.
- [54] B.M. Pettitt, P.J. Rossky, Alkali halides in water: ion-water correlations and ion-ion potentials of mean force at infinite dilution, *J. Chem. Phys.* 84 (1986) 5836.
- [55] A.S. Quist, W.L. Marshall, The electrical conductances of some alkali metal halides in aqueous solutions from 0 to 800 °C and at pressures to 4000 bar, *J. Phys. Chem.* 73 (1969) 978.
- [56] M.R. Reddy, M. Berkowitz, The dielectric constant of SPC/E water, *Chem. Phys. Lett.* 155 (1989) 173.
- [57] J.R. Reimers, R.O. Watts, M.L. Klein, Intermolecular potential functions and the properties of water, *Chem. Phys.* 64 (1982) 95.
- [58] R. Rey, E. Guardia, Dynamical aspects of the $\text{Na}^+ - \text{Cl}^-$ ion pair association in water, *J. Phys. Chem.* 96 (1992) 4712.
- [59] P.J. Rossky, The structure of polar molecular liquids, *Ann. Rev. Phys. Chem.* 36 (1985) 321.
- [60] B. Roux, The calculation of the potential of mean force using computer simulations, *Comp. Phys. Commun.* 91 (1995) 275.
- [61] J.P. Ryckaert, G. Ciccotti, H.J.C. Berendsen, Numerical integration of the cartesian equations of motion of a system with constraints: molecular dynamics of *n*-alkanes, *J. Comput. Phys.* 23 (1977) 327.
- [62] H. Sadek, R.M. Fuoss, Electrolyte-solvent interaction. VI. Tetra-butylammonium bromide in nitrobenzene-carbon tetrachloride mixtures, *J. Am. Chem. Soc.* 76 (1954) 5905.
- [63] H. Shinto, S. Morisada, M. Miyahara, K. Higashitani, A reexamination of mean force potentials for the methane pair and the constituent ion pairs of NaCl in water, *J. Chem. Eng. Jpn.* 36 (2003) 57.
- [64] V. Simonet, Y. Calzavara, J.L. Hazemann, R. Argoud, O. Geaymond, D. Raoux, X-ray absorption spectroscopy studies of ionic association in solutions of zinc bromide from normal to critical conditions, *J. Chem. Phys.* 117 (2002) 2771.
- [65] D.E. Smith, L.X. Dang, Computer simulations of NaCl association in polarizable water, *J. Chem. Phys.* 100 (1994) 3757.
- [66] P.E. Smith, B.M. Pettitt, Peptides in ionic solutions: a comparison of the Ewald and switching function techniques, *J. Chem. Phys.* 95 (1991) 8430.
- [67] P.E. Smith, B.M. Pettitt, Ewald artifacts in liquid state molecular dynamics simulations, *J. Chem. Phys.* 105 (1996) 4289.
- [68] M. Sprik, G. Ciccotti, Free energy from constrained molecular dynamics, *J. Chem. Phys.* 109 (1998) 7737.

- [69] G. Stell, G.N. Patey, J.S. Hoye, Ornstein–Zernike equation for a 2-yukama $C(R)$ with core condition, *Adv. Chem. Phys.* 48 (1981) 183.
- [70] G.M. Torrie, J.P. Valleau, Nonphysical sampling distributions in Monte Carlo free energy estimation: umbrella sampling, *J. Comput. Phys.* 23 (1977) 187.
- [71] E. Wasserman, B. Wood, J. Brodholt, The static dielectric constant of water at pressures up to 20 kbar and temperatures to 1273 K: experiment, simulations, and empirical equations, *Geochim. Cosmochim. Acta* 59 (1994) 1.
- [72] S. Winstein, E. Clippinger, A.H. Fainberg, G.C. Robinson, Salt effects and ion pairs in solvolysis, *J. Am. Chem. Soc.* 76 (1954) 2597.
- [73] L.V. Woodcock, Isothermal molecular dynamics calculations for liquid salts, *Chem. Phys. Lett.* 10 (1971) 257.
- [74] G.H. Zimmerman, M.S. Gruszkiewicz, R.H. Wood, New apparatus for conductance measurements at high temperatures: conductance of aqueous solutions of LiCl, NaCl, NaBr, and CsBr at 28 MPa and water densities from 700 to 260 kg m⁻³, *J. Phys. Chem.* 99 (1995) 11612.